ATMOSPHERIC MOTION VECTORS DERIVED FROM MSG RAPID SCANNING SERVICE DATA AT EUMETSAT

Manuel Carranza [1], Arthur de Smet [2], Jörgen Gustafsson [2]

[1] GMV Aerospace and Defence S.A. at EUMETSAT, Eumetsat-Allee 1, D-64295 Darmstadt, Germany
[2] EUMETSAT, Eumetsat-Allee 1, D-64295 Darmstadt, Germany

Abstract

EUMETSAT derives atmospheric motion vectors (AMVs) operationally from the imagery of three geostationary satellites: Meteosat-7 (sub-satellite longitude 57° E), Meteosat-8 (sub-satellite longitude 9.5° E), and Meteosat-9 (sub-satellite longitude 0°). The average dissemination rate for the latter is almost 40,000 winds per hour.

The Meteosat Second Generation (MSG) satellites (currently MSG-1 – known as Meteosat-8 – and MSG-2 – known as Meteosat-9) normally scan the full Earth disc every fifteen minutes. By scanning a smaller area scans can be conducted more frequently. This is known as rapid scanning. Presently the MSG Rapid Scanning Service (RSS) provides images of about one third of the full Earth disc every five minutes.

RSS delivers not only MSG image data but also a selection of advanced meteorological products, the most important of which is the AMV product. RSS from Meteosat-8 commenced on 13 May 2008 from a position at 9.5°E as a follow-on to the successful Meteosat-6 RSS, which ended in 2007.

In the present paper results obtained recently with Meteosat-8 in Rapid Scanning mode are discussed and compared with results from Meteosat-9 in Full-Earth Scanning (FES) mode, with special focus on results from the high resolution visible (HRVIS) winds. The possibility of using smaller target sizes for the derivation of operational AMVs is also presented.

GENERAL CHARACTERISTICS OF THE RAPID SCANNING SERVICE

The Meteosat Second Generation (MSG) satellites normally scan the full Earth disc every 15 minutes. By scanning a smaller area scans can be conducted more frequently. If only a third of the Earth disc is scanned, it takes a third of the time to scan the area - in this case every 5 minutes instead of every 15 minutes. This is known as rapid scanning.

Rapid Scanning Service (RSS) from Meteosat-8 commenced on 13 May 2008 from a position at 9.5ºE as a follow-on to Meteosat-6 RSS, which ended in 2007. RSS delivers MSG image data as well as a selection of advanced meteorological products.

The baseline scan region is an area that corresponds approximately to the top third of a nominal repeat cycle. The service generates data at 5-minute intervals. The rapid scan area for the MSG RSS covers a latitude range from approximately 15ºN to 70ºN for all 12 channels (see Figure 1).

RSS data dissemination is identical to normal data dissemination. Image segments are based on 464 lines, which are compatible with the full disc level 1.5 data scans. The calibration is identical to Full Earth Scanning (FES), whereas the image rectification is to 9.5ºE instead of 0º.

The RSS is periodically interrupted for short periods of time. These temporary outages are used to exercise the instrument mechanics in FES, which is required to keep the mechanism in good repair. In

addition, these periods are used for essential maintenance activities. During the period between rapid scanning sessions, meteorological products are not disseminated.
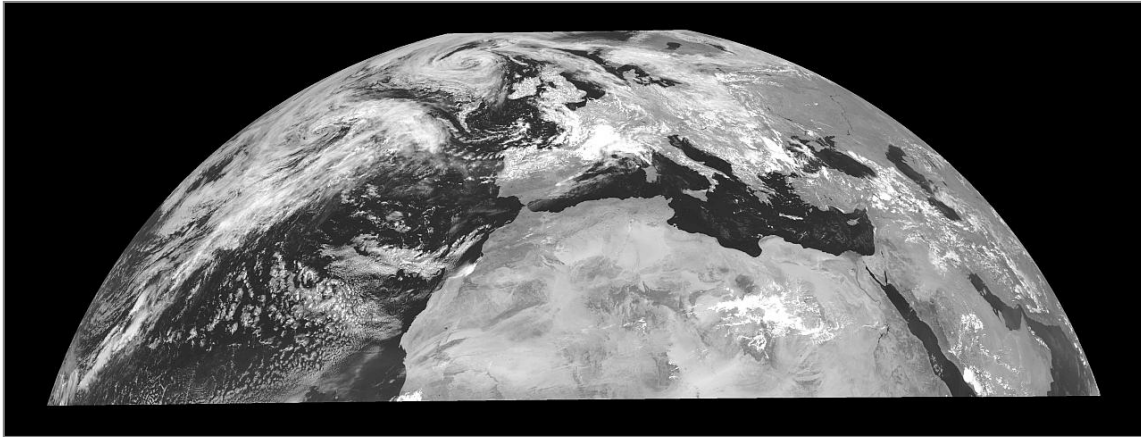
Figure 1: **Meteosat-8 rapid scan area.**

The baseline operational period for MSG RSS is 26 days of continuous rapid scanning followed by 2 days of full Earth disc scanning, over 11 months per year. The 12th month (around December and January) is devoted to either FES or no imaging. Additional interruptions to RSS can be expected if the equipment used to provide the service is needed to support the service of Meteosat-9 at 0⁰.

The distribution of the meteorological products generated from RSS data (see Table 1) is performed via EUMETCast and the GTS in the same way as for the nominal 0⁰ service products.

Product	Format	Frequency
Atmospheric Motion Vectors (AMV)	BUFR	Every 20 minutes
Clear Sky Radiances (CSR)	BUFR	Every 15 minutes
Multi-sensor Precipitation Estimate (MPE)	BUFR	Every 5 minutes
Active Fire Monitoring (FIRG)	GRIB	Every 5 minutes
Active Fire Monitoring (FIRA)	ASCII	Every 5 minutes
Global Instability Index (GII)	BUFR	Every 5 minutes

Table 1: **Meteorological products from RSS data.**

COMPARISON OF RAPID SCANNING (RSS) AND FULL-EARTH SCANNING (FES)

First a series of images from Meteosat-9 in Full Earth Scanning mode and Meteosat-8 in Rapid Scanning Service mode are shown. Then two specific cases are compared in order to show the benefits of RSS for different channels.

Full Earth Scanning images from Meteosat-9

Figures 2, 3, 4 and 5 show sequences of images from the visible 0.8 μm channel, the water vapour 6.2 μm channel, the infrared 10.8 μm channel and the high resolution visible (HRVIS) channel of Meteosat-9 in FES mode, respectively.

From Figures 2 and 5 it appears clear that for the visible channels winds cannot be derived in the shadowed part of the Earth disc. This is not the case for the water vapour and infrared channels, for which winds can be derived throughout the whole full Earth disc.
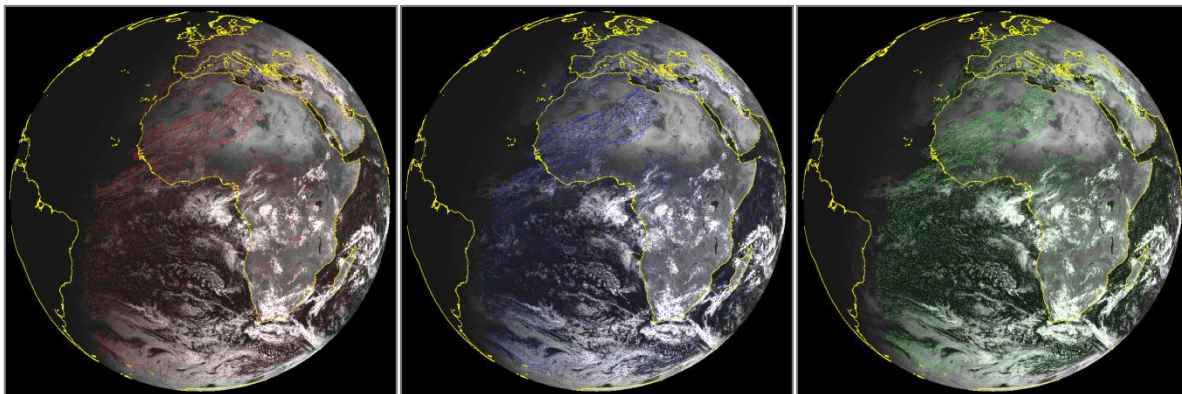
Figure 2: **VIS 0.8 μm full Earth disc (25/01/2010 - 08:15 to 08:45).**

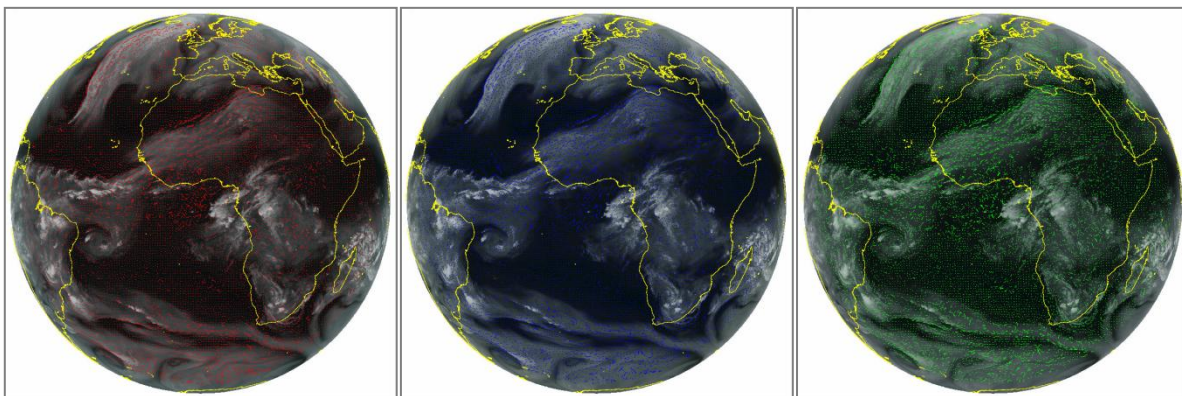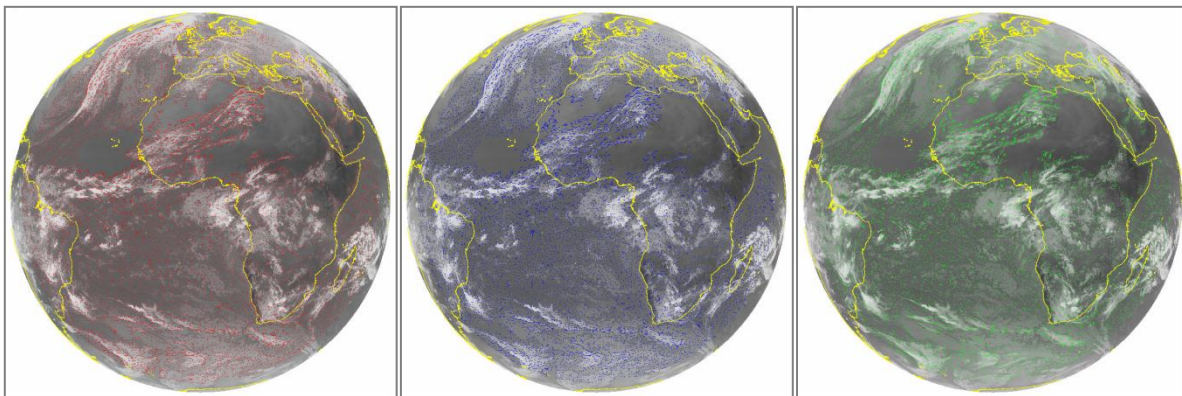*Figure 3:* **WV 6.2 μm full Earth disc (25/01/2010 - 08:15 to 08:45).**

Figure 4: **IR 10.8 μm full Earth disc (25/01/2010 - 08:15 to 08:45).**
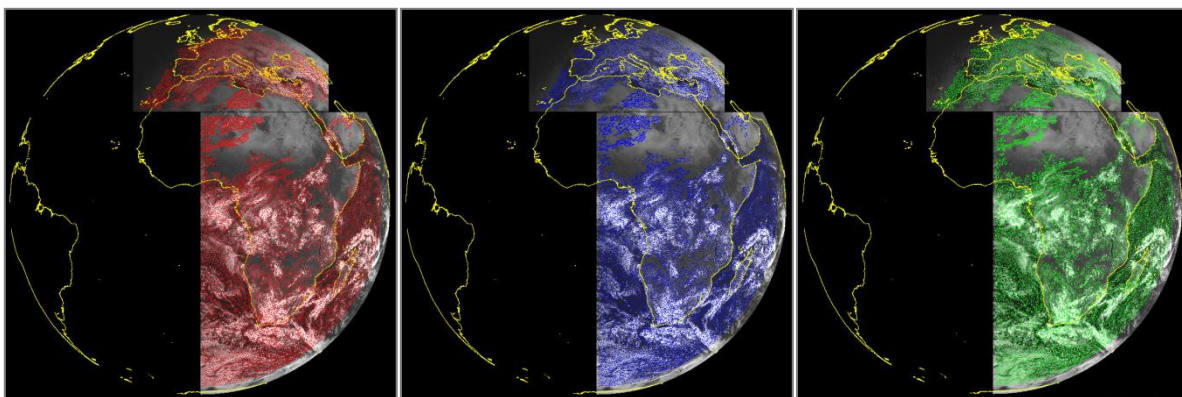

Figure 5: **HRVIS full Earth disc (25/01/2010 - 08:15 to 08:45).**

Rapid Scanning Service images from Meteosat-8

Figures 6, 7, 8 and 9 show sequences of images from the visible 0.8 μm channel, the water vapour 6.2 μm channel, the infrared 10.8 μm channel and the HRVIS channel of Meteosat-8 in RSS mode, respectively.

Again, from Figures 6 and 9 it appears clear that for the visible channels winds cannot be derived in the shadowed part of the scanned area, whereas for the water vapour and infrared channels winds can be derived throughout the whole scanned area.
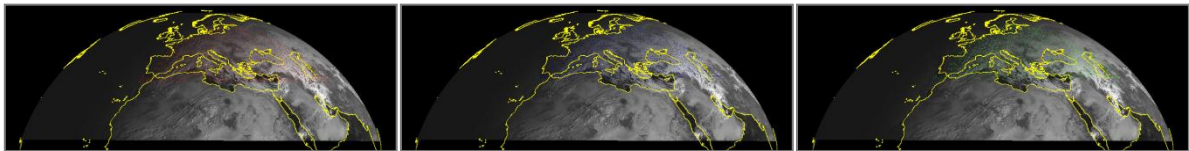

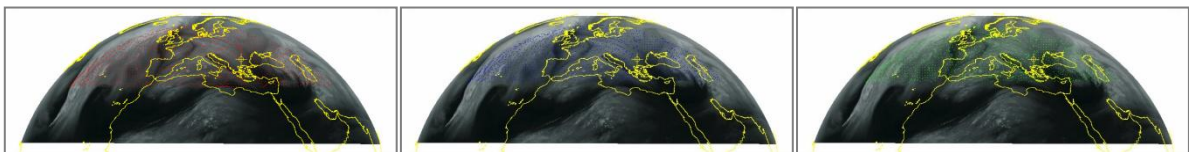*Figure 6:* VIS 0.8 μm rapid scan area (25/01/2010 - 08:05 to 08:15).

Figure 7: WV 6.2 μm rapid scan area (25/01/2010 - 08:05 to 08:15).

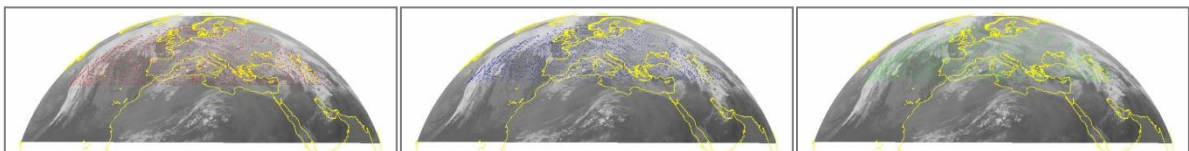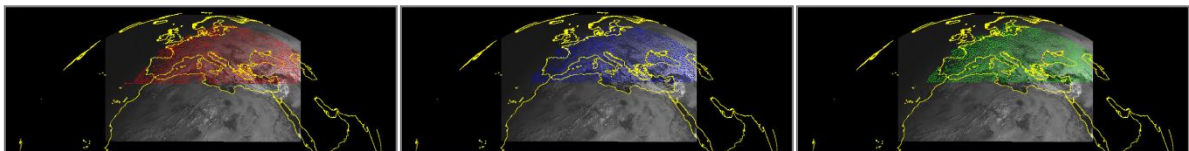*Figure 8:* IR 10.8 μm rapid scan area (25/01/2010 - 08:05 to 08:15).

Figure 9: HRVIS rapid scan area (25/01/2010 - 08:05 to 08:15).

Comparison of FES and RSS images

Figure 10 shows a sequence of images over the Azores islands from the water vapour 6.2 μm channel of Meteosat-9 in FES mode. Figure 11 shows the corresponding sequence of images from the water vapour 6.2 μm channel of Meteosat-8 in RSS mode. Only the best winds, with quality index above 90%, are shown.
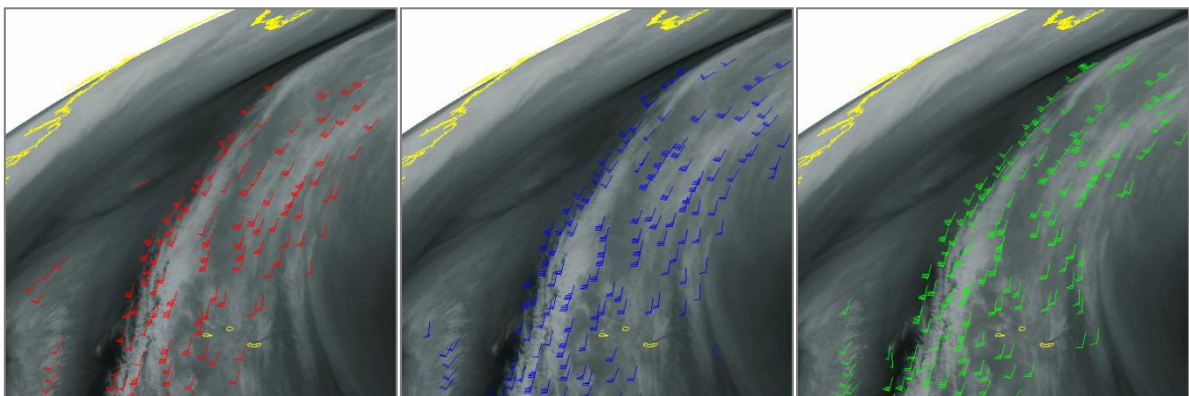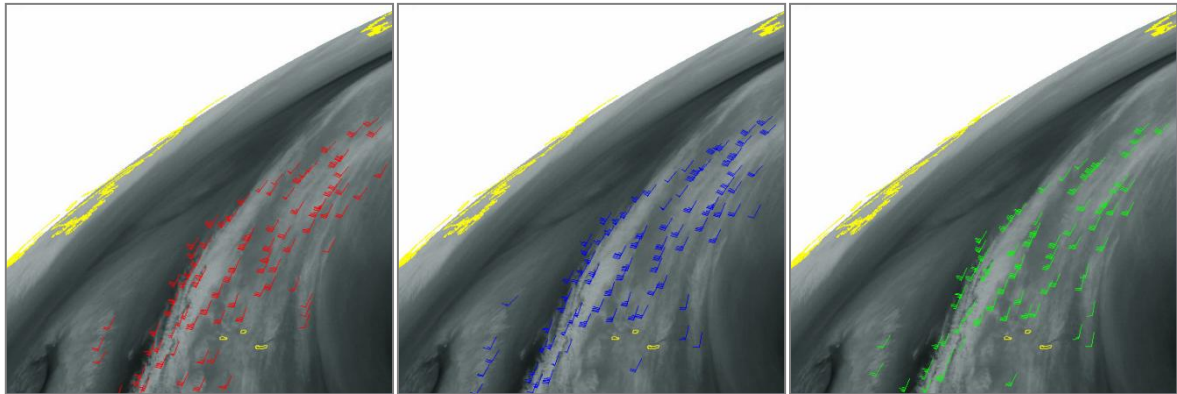

*Figure 10:* WV 6.2 μm FES images over the Azores islands (26/01/2010 - 10:15 to 10:45), QI > 90%.

Figure 11: **WV 6.2 μm RSS images over the Azores islands (26/01/2010 - 10:25 to 10:35), QI > 90%.**

It seems clear that using RSS for the water vapour channel does not provide any benefit with respect to FES in terms of an increased amount of good winds.

Figure 12 shows a sequence of images over the Black Sea from the high resolution visible channel of Meteosat-9 in FES mode. Figure 13 shows the corresponding sequence of images from the high resolution visible channel of Meteosat-8 in RSS mode. Again, only the best winds, with quality index above 90%, are shown.
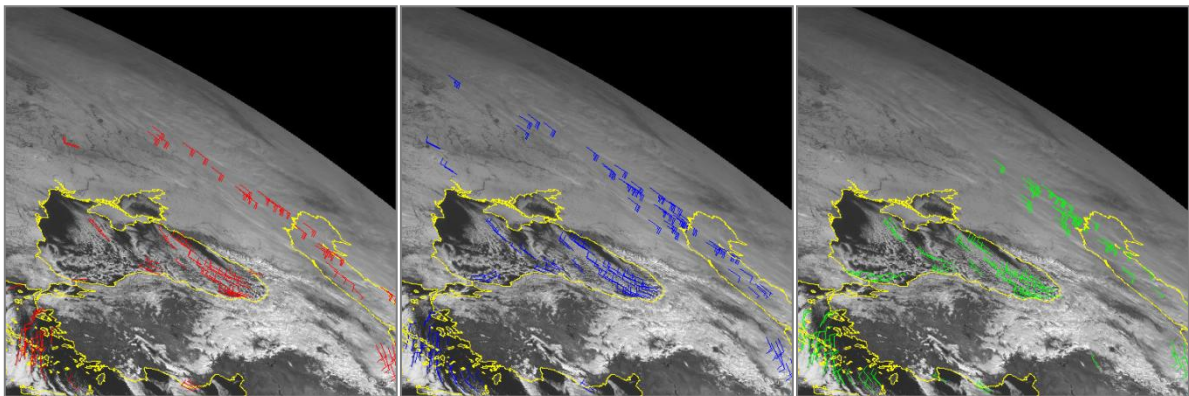
Figure 12: **HRVIS FES images over the Black Sea (26/01/2010 - 10:15 to 10:45), QI > 90%.**
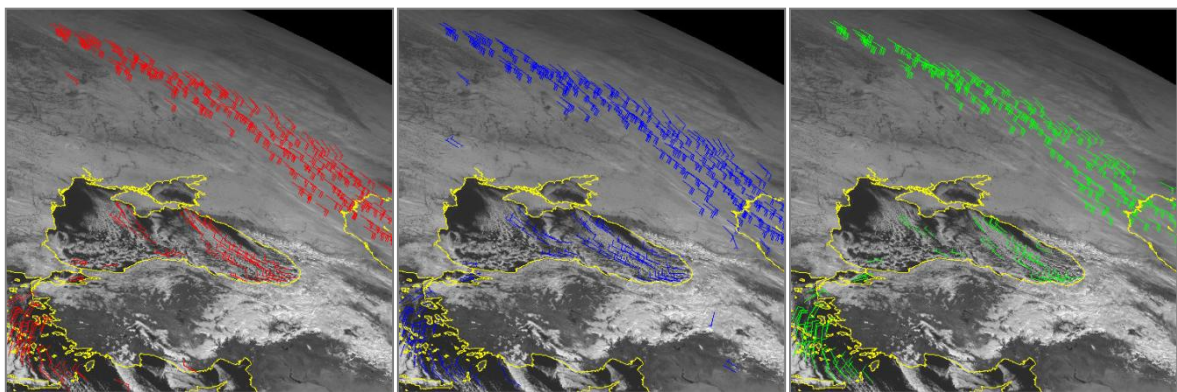
Figure 13: **HRVIS RSS images over the Black Sea (26/01/2010 - 10:25 to 10:35), QI > 90%.**

In this case, it seems clear that using RSS for the high resolution visible channel provides a great benefit with respect to FES, because the amount of good winds is significantly larger in the former case than in the latter.

Notice that, because Meteosat-9 is located at 0º and Meteosat-8 is located at 9.5ºE, the areas covered by both satellites are not exactly the same and a direct comparison is not completely consistent.

LIMITATIONS OF RSS

The main drawback of the wind derivation from RSS imagery is the inherent difficulty to track the motion of certain types of clouds, because many cloud systems do not move much in 5 minutes. Hence, due to the characteristics of the RSS, there is a limitation in the minimum wind speed that can be derived. Tables 2 and 3 show the value of the theoretical minimum wind speed derived from the pixel size, both at nadir and at 60⁰N, respectively.

Channel	Type	Pixel size at nadir	Corresponding wind speed	
			FES	**RSS**
1-11	VIS, WV, IR	3 km	3.3 m/s	10.0 m/s
12	HRVIS	1 km	1.1 m/s	3.3 m/s

Table 2: **Theoretical minimum wind speed as a function of pixel size at nadir.**

Channel	Type	Pixel size at 60⁰N	Corresponding wind speed	
			FES	**RSS**
1-11	VIS, WV, IR	6 km	6.6 m/s	20.0 m/s
12	HRVIS	2 km	2.2 m/s	6.7 m/s

Table 3: **Theoretical minimum wind speed as a function of pixel size at 60⁰N.**

Because an interpolation process is used for the pixels, it is possible to obtain sub-pixel accuracy in the motion of cloudy and clear-sky targets, so that the actual minimum wind speed achievable with RSS is significantly smaller than the values shown in Tables 2 and 3. In any case, there is an intrinsic limitation in the minimum detectable wind speed, which is much more restrictive than that for FES.

TESTS CARRIED OUT

In order to analyse the benefit of using RSS instead of FES several comparisons of RSS and FES data have been carried out. For that purpose, three different configurations have been used, namely:

- OPE-A: Current operational RSS;
- OPE-B: Current operational FES;
- VAL-A: Validation RSS.

Several different parameters have been used in the various configurations, the most important of which are shown in Table 4.

Parameter	Non-HRVIS		HRVIS	
	OPE-A	**VAL-A**	**OPE-A**	**VAL-A**
Target area size (pixels)	24	16	32	24
Search area size (pixels)	80	32	96	48

Table 4: **Parameters used in the various configurations.**

Figures 14 and 15 illustrate the differences in target area size between the operational configuration and the validation configuration for the non-HRVIS channels and the HRVIS channel, respectively. Because the pixel size is three times smaller for the HRVIS channel than for the non-HRVIS channels, a target area of 24 by 24 pixels effectively represents a much smaller area in the HRVIS case (see Figure 14 left and Figure 15 right).

The geographical area used for the comparison covers a latitude range from 36⁰N to 58⁰N, and a longitude range from 20⁰W to 45⁰E.

OPE-A, OPE-B and VAL-A data have been collected from 20 January 2010 to 5 February 2010, both

around noon and midnight. Due to the characteristics of the visible 0.8 μm channel and the HRVIS channel, data could only be collected around noon, so that the total amount of data from these channels used in the analysis is roughly half of that from the water vapour 6.2 μm channel and the infrared 10.8 μm channel.
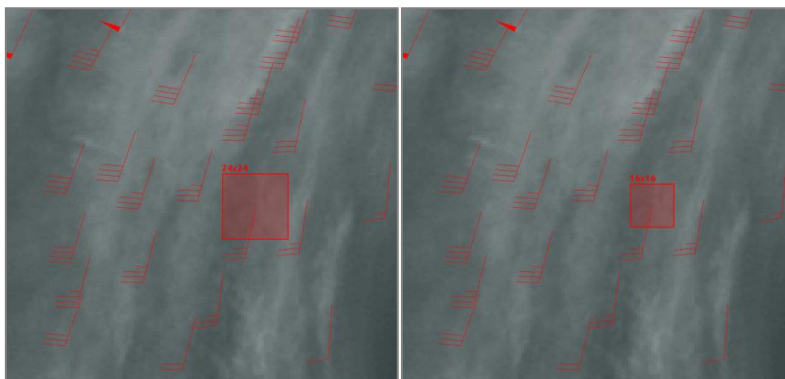

Figure 14: **Non-HRVIS OPE-A (left) and VAL-A (right) target area size comparison.**
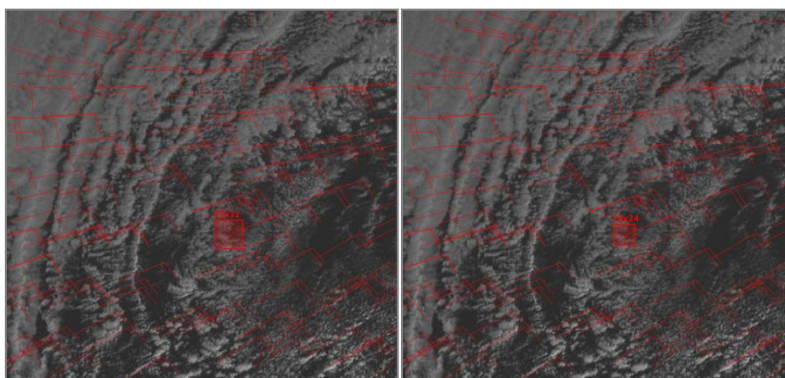

Figure 15: **HRVIS OPE-A (left) and VAL-A (right) target area size comparison.**

Additionally, a thorough complementary comparison of both FES and RSS data with radiosonde observations has been carried out, spanning between 18 December 2009 and 12 January 2010.

RESULTS AND STATISTICS

Forecast consistency

Figure 16.a shows a histogram of the forecast consistency for the operational FES results (OPE-A). The blue line represents all winds. The additional green, yellow and red lines represent only winds with a speed larger than 10 m/s, 20 m/s and 30 m/s, respectively.

In all cases, the shape of the histogram is very similar: there is a great amount of winds with forecast consistency below 20%, and then the amount of winds increases steadily with the forecast consistency, so that good winds are, in general, more frequent than poor winds. Furthermore, the larger the speed offset, the larger the amount of good winds (those with forecast consistency above 80%). This is an indication that, in general, the fastest winds have a better forecast consistency.

In the same fashion, Figure 16.b shows a histogram of the forecast consistency for the operational RSS results (OPE-B). The shape of the histogram is very similar to that of Figure 16.a, although an increase in the number of fast winds with forecast consistency above 80% is noticeable.
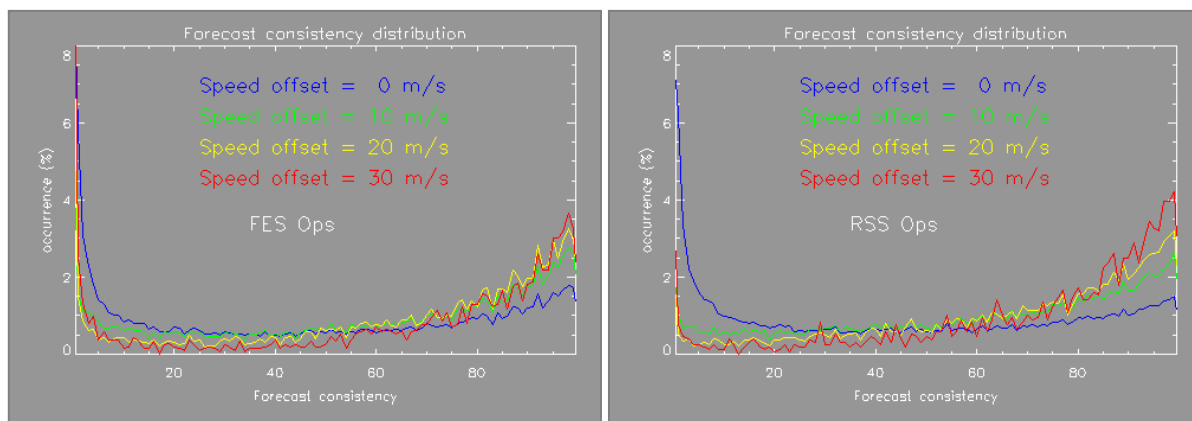
Figure 16: **(a) IR 10.8 μm operational FES wind forecast consistency (left);**
(b) IR 10.8 μm operational RSS wind forecast consistency (right).

If similar figures are generated for OPE-A, OPE-B and VAL-A, then it is possible to represent the average forecast consistency as a function of wind speed for all three configurations, which allows a direct comparison of the different methods considered.

Figures 17.a and 17.b show the average forecast consistency as a function of wind speed for the visible 0.8 μm channel and the water vapour 6.2 μm channel, respectively. It can be clearly appreciated that the average forecast consistency for RSS is approximately the same as for FES.

For the visible channel, the overall impact of RSS is neutral or slightly negative in general, and only slightly positive for very fast winds. For the water vapour channel, the overall impact is slightly negative. Besides, a reduction of the target area size (accounted for in the yellow lines, labelled as RSS test) does not have a clear positive impact in any of the cases. This is a clear indication that RSS does not provide any benefit for both visible and water vapour channels.
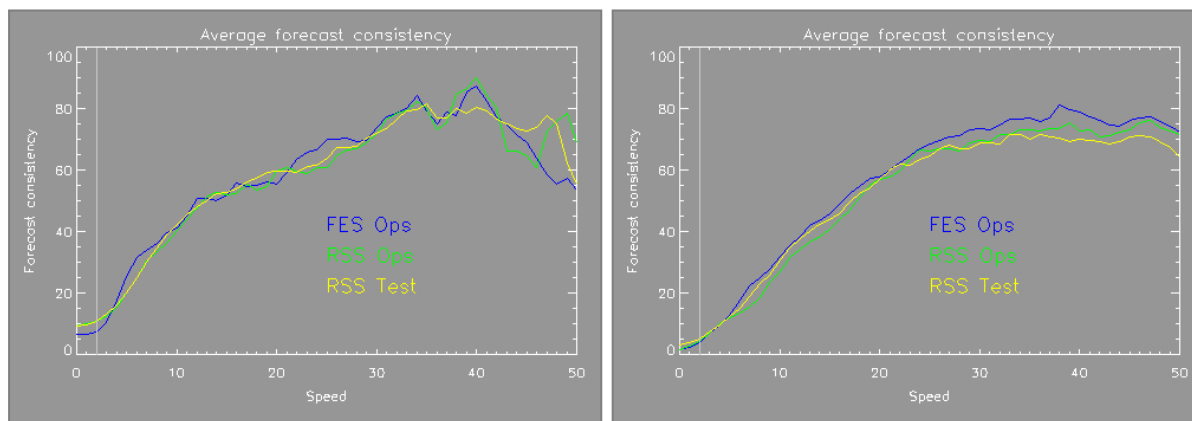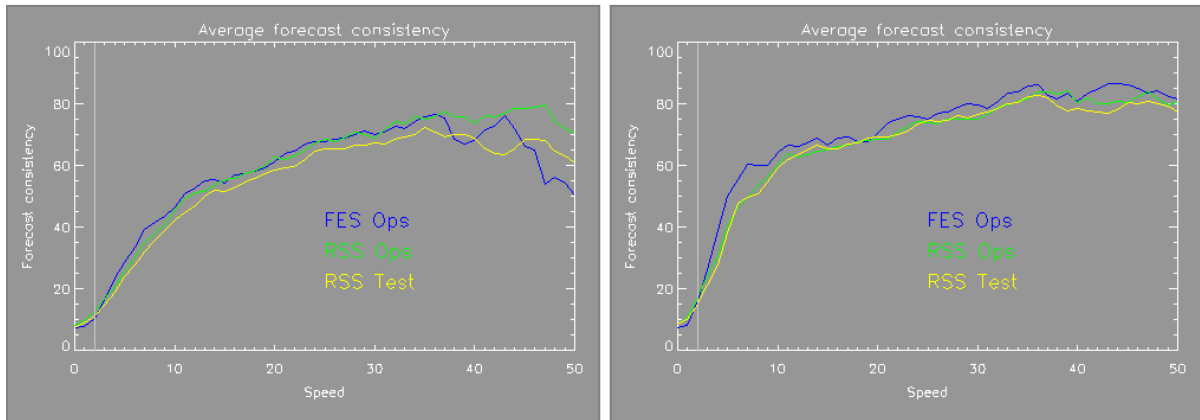

Figure 17: **(a) VIS 0.8 μm wind forecast consistency comparison (left);**
(b) WV 6.2 μm wind forecast consistency comparison (right).

Figure 18.a shows the average forecast consistency as a function of wind speed for the infrared 10.8 μm channel. In this case, the overall impact of RSS is slightly positive for fast winds, but neutral for winds slower than 35 m/s.

Figure 18.b also shows the average forecast consistency as a function of wind speed for the infrared 10.8 μm channel, but only winds with quality index above 80% are considered this time. Here the slightly positive impact of RSS for fast winds is lost, and the overall impact is slightly negative for all speeds. Reducing the target size (yellow line) does not seem to have a big impact.

In summary, for the infrared channel there is a slightly positive impact for fast winds, but only for those with quality index below 80%, which, however, are usually not considered by the user community.
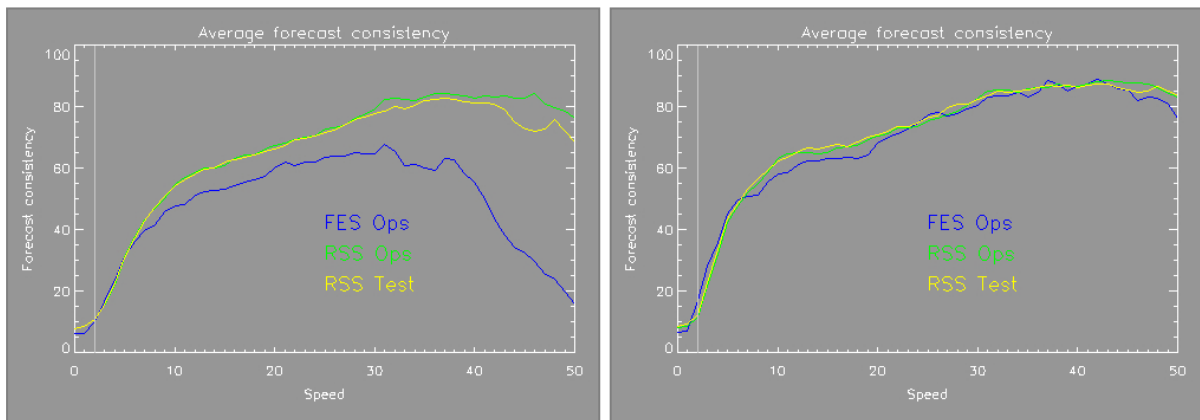
Figure 18: **(a) IR 10.8 μm wind forecast consistency comparison (left);**
(b) IR 10.8 μm wind forecast consistency comparison, QI > 80% (right).

Figure 19.a shows the average forecast consistency as a function of wind speed for the HRVIS channel. In this case, the overall impact of RSS is significantly positive for all winds, specially for those faster than 30 m/s.

Again, figure 19.b shows the average forecast consistency as a function of wind speed for the HRVIS channel, but only winds with quality index above 80% are considered this time. Here the big positive impact of RSS for all winds is lost, and the overall impact is neutral in general, and only slightly positive for slow and very fast winds. Once more, reducing the target size (yellow line) does not seem to have a big impact.

Figure 19: **(a) HRVIS wind forecast consistency comparison (left);**
(b) HRVIS wind forecast consistency comparison, QI > 80% (right).

In summary, for the HRVIS channel there is a big positive impact for all winds, specially significant for those with quality index below 80%. However, for the best winds the impact is neutral or just slightly positive.

Comparison with radiosonde observations

A comparison of the winds obtained from the different channels with radiosonde data yields many more collocations for RSS than for FES, specially for the HRVIS channel (see Table 5). The speed bias and the RMS error are very similar in both cases, although the values are slightly larger for RSS. In any case, the overall quality of the winds is very similar for RSS and FES for all channels.

This is an indication that HRVIS winds produced from RSS data are, in general, in better agreement with forecast data than those produced from FES data. This is not the case for other channels (visible, water vapour and infrared), for which the results are very similar.

Channel	Target type	Number of collocations			Speed bias (m/s)		RMS error (m/s)	
		FES	RSS	Δ(%)	FES	RSS	FES	RSS
VIS 0.8 μm	Cloudy	655	982	+49.9	−0.67	−1.14	5.84	6.31
WV 6.2 μm	Clear	222	182	−18.0	−1.78	−2.90	11.29	13.97
	Cloudy	16,180	16,866	+4.2	−3.01	−3.46	9.58	10.25
IR 10.8 μm	Cloudy	13,572	15,110	+11.3	−4.23	−4.87	9.83	10.59
HRVIS	Cloudy	3,700	7,721	+108.7	0.34	−0.19	6.05	6.47

Table 5: **Collocations with radiosonde observations.**

CONCLUSIONS

In terms of forecast consistency, the Rapid Scanning Service mode has a neutral impact in the generation of visible 0.8 μm winds, when comparing to Full-Earth Scanning mode. A reduction of the target area size does not improve this.

For water vapour 6.2 μm winds the impact is slightly negative. Besides, reducing the target area size does not bring anything positive.

In the case of infrared 10.8 μm winds, the impact is slightly positive for fast winds, although this small benefit is lost when taking into account only winds with quality index above 80%. Again, reducing the target size area does not have a positive impact.

More interestingly, for high resolution visible winds there is a large positive impact, specially for fast winds, with speed larger than 30 m/s. This big impact is almost completely diluted when considering only winds with quality index above 80%, but there is still a slightly positive impact for slow and very fast winds. Reducing the target area size has a neutral impact.

Concerning the comparison with radiosonde observations, RSS winds yield many more collocations than FES winds with similar quality.

All in all, it is convenient to use RSS for HRVIS winds, because:

- The overall impact, although small, is positive.
- The total amount of winds is larger if a smaller target area size is considered, which could prove useful for mesoscale studies.

Further analyses will be conducted in the near future in order to assess the results shown in the present paper. Special emphasis will be laid on the HRVIS channel, which seems to benefit the most out of the RSS.

REFERENCES

De Smet, A., (2002): "Operational AMV products derived with Meteosat-6 rapid scan data". Proceedings of the Sixth International Winds Workshop, Madison, WI, USA, pp. 179-185.

De Smet, A., Genkova, I., Forsythe, M. and Bormann, N., (2010): "The art of evaluating AMV algorithm changes". Proceedings of the Tenth International Winds Workshop, Tokyo, Japan.

Holmlund, K., van de Berg, L., Gustafsson, J., de Smet, A. and Borde, R., (2010): "Current status of EUMETSAT operational winds". Proceedings of the Tenth International Winds Workshop, Tokyo, Japan.